

EPR Spectra of α -1,2,3-[HPV(IV)V₂W₉O₄₀]⁶⁻, a Delocalized Mixed-Valence Compound

Hyunsoo So* and Chul Wee Lee

Department of Chemistry, Sogang University, Seoul 121-742. Received October 6, 1989

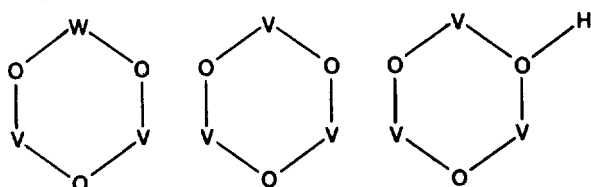
Solution and frozen solution EPR spectra of α -1,2,3-[HPV(IV)V₂W₉O₄₀]⁶⁻ have been analyzed. The isotropic hyperfine coupling constants remain constant at 350–77K, indicating that the unpaired electron is delocalized over three vanadium atoms probably even in the ground state.

Introduction

Mixed-valence heteropolyanions containing vanadium (IV) and vanadium (V) show a variety of interesting EPR spectra. So far four types of solution spectra have been observed: a 15-line spectrum for α -1,2-[SiV(IV)VW₁₀O₄₀]⁷⁻, [P₂V(IV)VW₁₆O₆₂]⁹⁻, and α -1,2-[PV(IV)VW₁₀O₄₀]^{6-,1-3} a 22-line spectrum² for [P₂V(IV)V₂W₁₅O₆₂]¹⁰⁻; a 36-line spectrum² for [HP₂V(IV)V₂W₁₅O₆₂]⁹⁻; and a 43-line spectrum¹ for α -1,2,3-[HSiV(IV)V₂W₉O₄₀]⁷⁻.

These compounds, represented in the abbreviated form below, may be classified in the following way:

(1) Compounds with edge-shared VO₆ octahedra

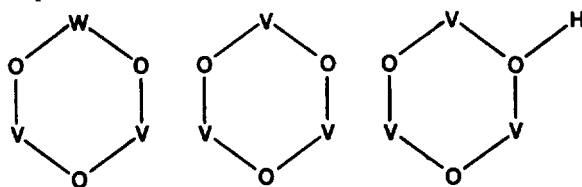


No. of lines: 15

22

36

(2) Compounds with corner-shared VO₆ octahedra



No. of lines: 15

(not prepared)

43

The multi-line pattern of each spectrum indicates that the unpaired electron interacts with more than one ⁵¹V nucleus (*I* = 7/2). The question arises whether these EPR spectra originate from a thermally-activated electron hopping process or a ground state delocalization. For a system with a hopping electron, the transition probability for the intramolecular electron transfer decreases as the temperature is lowered, and finally the electron is trapped on a single vanadium atom. The EPR spectrum of such a system is strongly dependent on the temperature, and it can be simulated using the modified Bloch equations.⁴ All four types of solution spectra could indeed be simulated on the basis of a hopping electron model.⁵ However, the resulting transition probabilities were much larger than the hyperfine coupling constants. When the unpaired electron is hopping very fast, the EPR spectrum can not be distinguished from that of a

delocalized system. Therefore we are unable to say whether the electron is rapidly hopping or delocalized on the basis of the solution EPR spectra for these mixed-valence complexes; the low temperature spectra should be analyzed.

The polycrystalline EPR spectra of all edge-shared complexes show that the unpaired electron is trapped on one vanadium atom at low temperatures.² And the polycrystalline spectrum of the corner-shared α -1,2,3-[H₂PV(IV)V₂W₉O₄₀]⁵⁻ doped into a diamagnetic host reveals clearly the temperature-dependence characteristic of electron hopping.⁶ This diprotonated species is equivalent to α -1,2-[PV(IV)VW₁₀O₄₀]⁶⁻ and α -1,2-[SiV(IV)VW₁₀O₄₀]⁷⁻ as far as the EPR spectrum is concerned, for the protonated bridging oxygen atoms prevent the electron transfer effectively. The latter compounds, not being very stable in solution, always show some impurity lines in their polycrystalline EPR spectra. But the main spectrum was the same as that of [H₂PV(IV)V₂W₉O₄₀]⁵⁻. Thus all compounds except the species showing the 43-line solution spectrum can be adequately described by the hopping electron model.

The polycrystalline spectra of corner-shared α -1,2,3-[HSiV(IV)V₂W₉O₄₀]⁷⁻ (HSiV₃)¹² and α -1,2,3-[HPV(IV)V₂W₉O₄₀]⁶⁻ (HPV₃) show no significant temperature dependence down to 77K, indicating that these compounds may be delocalized systems in their ground states. We have found that both solution and polycrystalline spectra of these compounds can be simulated reasonably using the delocalization model. Details are reported in this paper.

Experimental

Preparation of Compounds. α -1,2,3-K₈[PV₃W₉O₄₀] was prepared according to the method of Domaille.⁷ A solution of this compound in pH 4.7 acetate buffer was reduced to one-electron reduction state by adding hydrazine dihydrochloride.

EPR Measurements. EPR spectra were recorded on a Bruker EPR spectrometer (Model ER 200E) operating at 9.7 GHz. The microwave frequency was measured by a Hewlett-Packard frequency counter and DPPH was used as a g-marker. The frozen solution spectra were measured using 1:1 ethyleneglycol-water glass.

Results

Solution Spectra. The solution spectrum of HPV₃ at 80°C is shown in Figure 1. It looks similar to the 43-line spectrum of HSiV₃, but the intensity distribution is some-

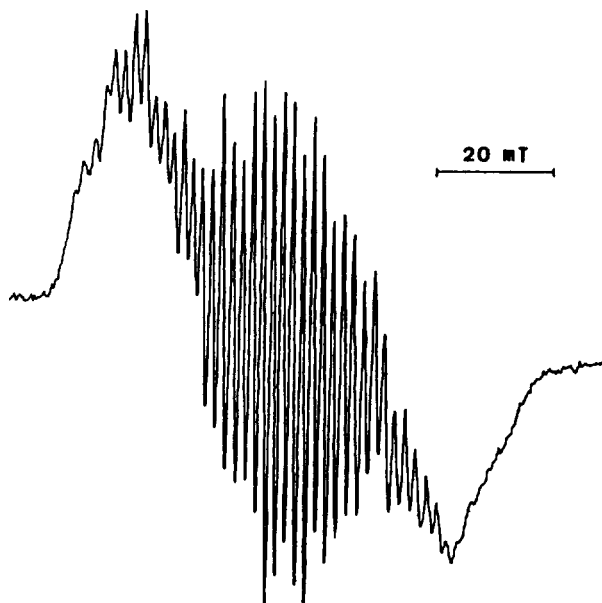


Figure 1. The solution EPR spectrum of α -1,2,3-[HPV(IV) $V_2W_9O_{40}$] $^{6-}$ at 80°C.

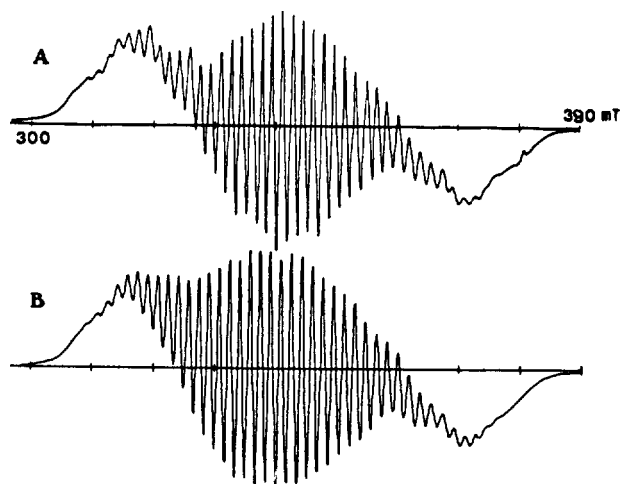


Figure 2. (A) The experimental and (B) simulated EPR spectra of α -1,2,3-[HSiV(IV) $V_2W_9O_{40}$] $^{7-}$ at 80°C. The Lorentzian line shape and the line width parameters $c = 0.88$, $d = -0.086$, and $f = 0.181$ mT were used in the simulation.

what different. The 43-line pattern was interpreted on the basis of the delocalization model.¹ Since one bridging oxygen atom is protonated, there are two kinds of vanadium atoms, a unique atom and two equivalent ones. Thus eight hyperfine lines (hyperfine coupling constant, a_1) by the unique vanadium atom will be split into 15 lines (hyperfine coupling constant, a_2) each by two equivalent vanadium atoms. If a_1/a_2 is approximately 4, a 43-line pattern is obtained.

The positions of the hyperfine lines could be calculated using the following spin Hamiltonian:

$$\hat{H} = g\beta B \cdot S + a_1 S \cdot I_1 + a_2 S \cdot (I_2 + I_3) \quad (1)$$

The intensity distribution was more difficult to simulate. For ordinary oxovanadium complexes, the line width W is

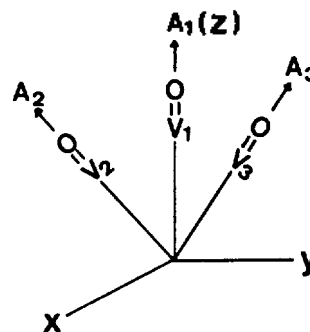


Figure 3. The orientations of three $V=O$ vectors in α -1,2,3-[HPV(IV) $V_2W_9O_{40}$] $^{6-}$. The angle between any two $V=O$ vectors is 38°. One of the principal axes of each hyperfine tensor is assumed to lie along the $V=O$ vector.

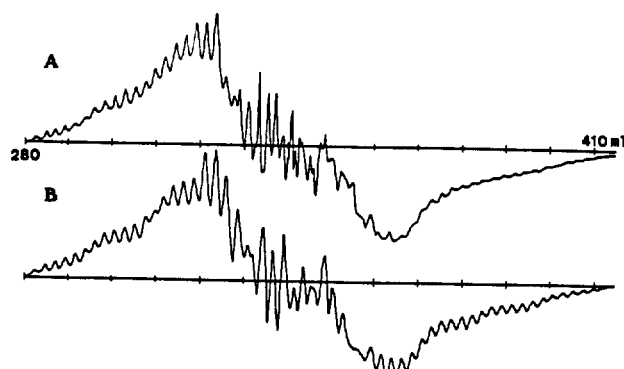


Figure 4. (A) The experimental and (B) simulated frozen solution EPR spectra of α -1,2,3-[HPV(IV) $V_2W_9O_{40}$] $^{6-}$ at 150K. The Lorentzian line shape and a line width of 1.0 mT were used in the simulation.

known to vary according to the formula

$$W = c + dm + fm^2, \quad (2)$$

where m is $-I, -I+1, \dots, +I$, and c, d , and f are the line width parameters. For the systems considered here, each hyperfine line is related to three hyperfine states. Eq. (2) was used to calculate the line width for each hyperfine state, and the average value for the three hyperfine states was used in the simulation.

The resulting pattern is in fair agreement with the spectrum of $HSiV_3$ as shown in Figure 2. The experimental spectrum of HPV_3 deviates more from this pattern, indicating that the dependence of the line width on m is more complex. However, the positions of the hyperfine lines for HPV_3 can be simulated reasonably. The resulting parameters are $g = 1.960$, $a_1 = 0.0063$,¹³ and $a_2 = 0.0015 \text{ cm}^{-1}$ for $HSiV_3$, and $g = 1.960$, $a_1 = 0.0064$, $a_2 = 0.0015 \text{ cm}^{-1}$ for HPV_3 .

Polycrystalline Spectra. A frozen solution EPR spectrum of HPV_3 is shown in Figure 3(A). The spectrum consisting of 57 parallel lines is unchanged between 200 and 77K. A similar spectrum with slightly different intensity distribution was observed for $HSiV_3$.

In order to simulate this spectrum we consider a model system consisting of three $V=O$ groups; see Figure 4. The unique $V=O$ group lies along the z axis, and the two equivalent $V=O$ groups cant away from this and from each other

by about 38%.⁹ The EPR spectrum of this system may be described by the following spin Hamiltonian:

$$\hat{H} = \beta B \cdot g \cdot S + S \cdot A_1 \cdot I_1 + S \cdot A_2 \cdot I_2 + S \cdot A_3 \cdot I_3 \quad (3)$$

The g and A_1 tensors may be assumed to be axial with coincident principal axes. The A_2 and A_3 tensors may also be assumed to be axial with the largest component along each $V = O$ vector. Fifty-seven parallel lines can be obtained when the hyperfine splitting for V_1 is 6 times as large as that of V_2 (or V_3) when the magnetic field is along the z axis. This shows that the hyperfine interaction with V_2 or V_3 is much smaller than that with V_1 .

Perturbation theory gives the following expressions for the angular dependence of the g value and the hyperfine coupling constant for V_1 ¹⁰

$$h\nu = g\beta H + K_1 m_i + \frac{B_1^2}{4g\beta H} \left(\frac{A_1^2 + K_1^2}{K_1^2} \right) \{I(I+1) - m_i^2\} \\ + \frac{1}{2g\beta H} \left(\frac{A_1^2 - B_1^2}{K_1} \right)^2 \left(\frac{g_{\parallel}^2 g_{\perp}^2}{g^4} \right) \sin^2 \theta \cos^2 \theta m_i^2 \quad (4)$$

where θ is the angle between the z axis and the magnetic field and

$$g^2 = g_{\parallel}^2 \cos^2 \theta + g_{\perp}^2 \sin^2 \theta \quad (5)$$

and

$$K_1^2 g^2 = A_1^2 g_{\parallel}^2 \cos^2 \theta + B_1^2 g_{\perp}^2 \sin^2 \theta \quad (6)$$

The angular dependence of the last two terms in Eq. (3) is difficult to express in simple equations because the principal axes of these hyperfine tensors do not coincide with those of the g tensor. Since these terms are small and the g anisotropy is not very large, we may use the following expression applicable when g is isotropic

$$K_i^2 = A_i^2 \cos^2 \chi + B_i^2 \sin^2 \chi \quad (i=2 \text{ or } 3), \quad (7)$$

where χ is the angle between the $V = O$ vector and the magnetic field for V_2 and V_3 .

The experimental and calculated spectra are compared in Figure 3. The outer lines could be simulated reasonably, but some lines in the central portion of the spectrum did not match those in the measured spectrum. This may be due to the anisotropy in A tensors neglected in this simulation. The resulting parameters are¹³

$$g_{\parallel} = 1.940, \quad g_{\perp} = 1.969$$

$$A_1 = 0.01245, \quad B_1 = 0.0040, \quad A_2 = 0.00245, \quad B_2 = 0.0010 \text{ cm}^{-1}.$$

Discussion

Isotropic hyperfine Coupling Constants. Both the solution and polycrystalline EPR spectra of HPV₃ could be simulated on the basis of a delocalized electron model. It is of interest to compare the isotropic hyperfine coupling constants determined from the two spectra. The values from the polycrystalline spectrum are $a_1 = 0.0068 \text{ cm}^{-1}$ and $a_2 = 0.0015 \text{ cm}^{-1}$, which are quite close to the values determined from the

solution spectrum at 80°C. Since hyperfine coupling constant is a measure of the unpaired electron density at vanadium atoms, this result shows that the unpaired electron density on each vanadium atom remains almost constant in the temperature range 350–77K. This is consistent with the delocalized electron model. Of course, we cannot exclude the possibility that the unpaired electron is trapped below 77K. If it were completely trapped at 10K, for example, the estimated activation energy is 140 cal/mol (50 cm⁻¹). In the absence of experimental data below 77K, we can say that the electron is completely delocalized or if it is hopping, the activation energy is very small.

Molecular Structure and Electron Transfer Rates.

Low-temperature EPR spectra of the heteropolyanions containing vanadium (IV) and vanadium (V) show that the electron transfer rates vary considerably depending upon the molecular structure. At 100K the unpaired electron is trapped on one vanadium atom when the VO₆ octahedra are edge-shared, while it is hopping in [H₂PV(IV)V₂W₉O₄₀]⁵⁻ and delocalized in [HPV(IV)V₂W₉O₄₀]⁶⁻ when the VO₆ octahedra corner-shared. As was pointed out by Pope, *et al.*,² the V–O–V angle plays an important role in the electron transfer. The unpaired electron on V⁴⁺ occupies the 3d_{xy} orbital which has π symmetry with respect to the bridging V–O bonds. Two 3d_{xy} orbitals in the V–O–V group overlap via the p _{π} orbital of the bridging oxygen atom. Since the V–O–V angle is 158° in the compounds with corner-shared VO₆ octahedra,⁹ a p _{π} orbital is available for considerable extent of d _{π} –p _{π} –d _{π} overlap. In the compounds where the VO₆ octahedra are edge-shared, the V–O–V angle is 125°¹¹ and the non-bonding orbitals of the bridging oxygen atom are close to the sp³ orbital. Therefore, the extent of d _{π} –p _{π} –d _{π} overlap is low, and the electron is trapped on a single vanadium atom at high temperatures. A similar argument can be applied to the protonated bridging oxygen atom, which prevents the electron transfer effectively even at room temperature. When the bridging oxygen is protonated, it seems that d _{π} –p _{π} –d _{π} overlap is negligible and the electron transfer is completely prevented.

We have shown that the species α -1,2,3-[HPV(IV)V₂W₉O₄₀]⁶⁻ and α -1,2,3-[HSiV(IV)V₂W₉O₄₀]⁷⁻ are delocalized systems quite probably in their ground states. It is interesting to note that the extent of electron trapping is quite different depending upon the molecular structure, and this may increase the usefulness of heteropolyanions in elucidating the mechanism of electron transfer in mixed-valence compounds.

Acknowledgement. The support of this research by the Ministry of Education is gratefully acknowledged.

References

1. M. M. Mossoba, C. J. O'Connor, M. T. Pope, E. Sinn, G. Herve and A. Teze, *J. Am. Chem. Soc.*, **101**, 6864 (1980).
2. S. P. Harmaker, M. A. Leparulo and M. T. Pope, *J. Am. Chem. Soc.*, **105**, 4286 (1983).
3. C. W. Lee, H. So, and K. R. Lee, *Bull. Korean Chem. Soc.*, **7**, 39 (1986).
4. H. So, *Bull. Korean Chem. Soc.*, **8**, 111 (1987).
5. H. So, C. W. Lee and D. Lee, *Bull. Korean Chem. Soc.*, **8**,

- 384 (1987).
6. C. W. Lee and H. So, *Bull. Korean Chem. Soc.*, **7**, 318 (1986).
 7. P. J. Dommelle, *J. Am. Chem. Soc.*, **105**, 4286 (1983).
 8. See, for example, R. Wilson and D. Kivelson, *J. Chem. Phys.*, **44**, 154 (1966).
 9. F. Robert, A. Teze, G. Herve, and Y. Jeannin, *Acta Cryst.*, **B36**, 11 (1980).
 10. B. Bleaney, *Phil. Mag.*, **42**, 441 (1951).
 11. B. Dawson, *Acta Cryst.*, **6**, 113 (1953).
 12. Low temperature EPR spectra of HSiV_3 were mentioned in ref. 1, but details have not been published.
 13. The sign of the hyperfine coupling constants for the oxovanadium complexes are known to be minus (ref. 8), but it has been neglected in this paper.

An XPS Study of YBaCuO Compounds

Myung-Mo Sung and Yunsoo Kim*

Inorganic Chemistry Division, Korea Research Institute of Chemical Technology, Taejeon, 305-606

Received October 23, 1989

X-ray photoelectron spectra have been obtained and comparisons have been made for 1-2-3 and 2-1-1 phases of YBaCuO compounds. The photoelectron binding energies of all the constituent elements are consistently larger for the 2-1-1 phase than for the 1-2-3 phase. The peak intensities reflect different stoichiometries of the two phases. For the superconducting 1-2-3 phase, its degradation in air and interaction with water and carbon dioxide were examined by taking core level spectra of all the elements. It appears that yttrium is the most affected by exposure to air, since it undergoes a rapid change to carbonate when water and subsequently carbon dioxide are introduced.

Introduction

Since the discovery of YBaCuO superconductor with T_c higher than 90K, efforts have been made to elucidate the crystal and the electronic structures of the superconducting material. The study of the electronic structures of this high temperature superconductor by use of X-ray photoelectron spectroscopy has contributed much to the explanations of various phenomena such as the superconducting mechanism, effect of temperature,^{1,2} and degradation in air.³ As is well known, the YBaCuO superconductor is quite unstable in air, which will cause difficulties in its utilization. For the application of YBaCuO superconductor to be successful, it is necessary to understand its degradation mechanism. To this end, a careful examination of the changes of the superconductor surfaces is required.

The nonsuperconducting 2-1-1 phase has rarely been studied by XPS, but since it is often formed during the preparation of the 1-2-3 phase and is also considered to be a good candidate substrate for the 1-2-3 phase film, it will be quite informative to investigate the spectral differences between this phase and the superconducting 1-2-3 phase. In this study, the core orbital binding energies of the elements in 1-2-3 and 2-1-1 phases of YBaCuO compounds were determined and compared. To investigate the degradation mechanism of the 1-2-3 phase in air, spectral changes of the material were examined with time it was kept in air. The interaction of the material with water and carbon dioxide was also studied.

Experimental

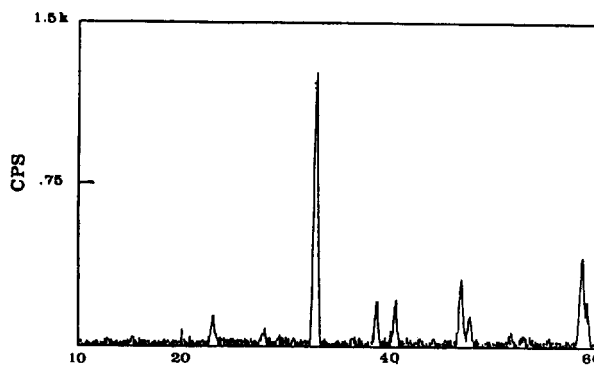


Figure 1. XRD pattern of $\text{YBa}_2\text{Cu}_3\text{O}_{7-x}$.

To prepare the 1-2-3 phase, $\text{YBa}_2\text{Cu}_3\text{O}_{7-x}$, we used $\text{YBa}_2\text{Cu}_3\text{O}_{6.5}$ powders purchased from Aldrich Chemical Company, Inc. without purification. The powders were pressed into pellets at 13600 psi. The pellets were then sintered at 950°C in flowing oxygen for 2 hours. From X-ray diffraction pattern of the sintered body, it was found to consist of the 1-2-3 single phase only (Figure 1). The 2-1-1 phase was made by pressing the equimolar mixture of Y_2O_3 , $\text{Ba}(\text{OH})_2$, and CuO powders into pellets at 13500 psi followed by calcination at 900°C for 18 hours and sintering at 940°C for 24 hours.⁴ The phase of the final product was confirmed to be 2-1-1, also by XRD as shown in Figure 2.

The samples thus prepared were transferred into the fast entry airlock of the ESCALAB MK II (VG Scientific Ltd.) and scraped by a diamond file to expose clean surfaces. The pressure of the airlock was maintained at 10^{-8} torr during